Bonding Polyether onto ZnO Nanoparticles: An Effective Method for Preparing Polymer Nanocomposites with Tunable Luminescence and Stable Conductivity**

By *Huan-Ming Xiong*, *Zi-Dong Wang*, *Da-Peng Liu*, *Jie-Sheng Chen*, *Yong-Gang Wang*, and *Yong-Yao Xia**

A series of new polymer nanocomposites, ZnO(PEGME), in which ZnO nanoparticles and poly(ethylene glycol methyl ether) (PEGME) molecules are connected by covalent bonds, have been synthesized by a sol–gel route and purified by a non-solvent method. Various characterization techniques have been employed to determine the compositions and structures of the ZnO(PEGME)s, and their luminescent properties and ionic conductivities (after dissolving lithium salts to form solid polymer electrolytes) have been measured and compared with their counterparts—polymer nanocomposites prepared by mixing PEGME and ZnO nanoparticles physically. These comparisons prove that ZnO(PEGME) hybrids derived from chemical reactions have much better properties and stabilities than their counterparts. As a result, tunable photoluminescence of ZnO nanoparticles and stable conductivity of solid polymer electrolytes have been realized successfully.

1. Introduction

Nanomaterials are an exciting subject in the fields of both fundamental study and applied science.[1] Recent research has not been limited to quantum dots, nanorods, nanotubes, and other simple nanostructures, but has progressed to nanocomposite materials with various structures and multiple functions.[2] Among the cooperative candidates for constructing nanocomposites, polymers are the best choice, because polymers have many complementary merits, such as elasticity, viscosity, and plasticity, that inorganic nanocrystals lack. Therefore, polymer nanocomposite materials have attracted extensive interest in the past decade.[3] Various polymer nanocomposites, including photonic crystals[4] and intercalative materials,[5] have been produced and investigated. In general, polymer nanocomposites can be prepared in two ways. One way is by physical methods, that is, mixing polymers and nanostructured materials by solid grinding, soaking in liquids, or gas diffusion.[6] In these physical mixtures, polymers and nanoparticles are connected by static interactions, van der Waals' forces, or Lewis acid–base interactions. The other way is by chemical reaction, that is, bonding polymers and nanostructured materials chemically.[7] Although physical methods are easy to handle and have been reported widely, chemical approaches are expected to produce more varied composites, owing to the diversity of chemical synthesis and the fact that the products are more stable because of stronger interactions between the components.

Recently, we reported that ZnO nanoparticles with acetate surface groups, designated ZnO(Ac), could enhance polyethylene oxide (PEO)–$LiClO_4$ film conductivity, and IR analyses proved that the PEO–Li^+–Ac(ZnO) bridge bonds prevented the electrolyte from crystallizing.[8] We found that the interactions between ZnO nanoparticles and PEO (MW = 600 000) made the ZnO photoluminescence (PL) stronger and blue-shifted. Later, Abdullah and co-workers found that, when ZnO nanoparticles were synthesized in a PEO/ethanol slurry, the dried product mixture emitted blue fluorescence and exhibited 10^{-6} S cm^{-1} conductivity after thermal treatment.[9] However, this polymer nanocomposite is simply a physical mixture of conventional ZnO(Ac) nanoparticles and PEO macromolecules. It was not stable during storage, and the blue ZnO nanoparticles, which were actually protected by excess LiOH in solution but not protected by PEO against agglomeration, could not be purified by the non-solvent method because LiOH would be washed away by the solvent. Furthermore, the conductivity of such a polymer-nanocomposite electrolyte after thermal treatment is mesostable, because the interactions between ZnO nanoparticle filler and polymer electrolytes are weak and depend on the thermal history.

Herein, we report a simple route for preparing pure polyether-grafted ZnO nanoparticles that are gels or waxes at room temperature. By controlling the particle sizes, the ZnO(PEGME) (PEGME = poly(ethylene glycol methyl ether)) PL can be tuned from blue to yellow. The ZnO(PEGME) sols have stronger and more stable luminescence than mixtures of PEGME and conventional ZnO(Ac) colloids with the same concentrations, and the optimal samples have quantum yields of over 30 %. Further-

[*] Prof. Y.-Y. Xia, Dr. H.-M. Xiong, Z.-D. Wang, Y.-G. Wang
Shanghai Key Laboratory of Molecular Catalysis and Innovative Materials, and Department of Chemistry
Fudan University
Shanghai 200433 (P.R. China)
E-mail: yyxia@fudan.edu.cn
Dr. D.-P. Liu, Prof. J.-S. Chen
State Key Laboratory of Inorganic Synthesis and Preparative Chemistry
College of Chemistry, Jilin University
Changchun 130012 (P.R. China)

[**] This work was supported by the National Natural Science Foundation of China.

 DOI: 10.1002/adfm.200500167

more, when $Li[N(CF_3SO_2)_2]$ is dissolved into ZnO(PEGME350) hybrids (where 350 denotes the molecular weight of PEGME), the resulting gels (excluding any solvent) have stable conductivities of over 10^{-4} S cm^{-1} at room temperature.

2. Results and Discussion

Figure 1 presents four high-resolution transmission electron microscopy (HRTEM) images of ZnO(PEGME350) samples. Because the ZnO(PEGME) hybrids are apt to decompose under intense electron beams, images with higher resolution are unavailable. The average particle diameters of the four samples

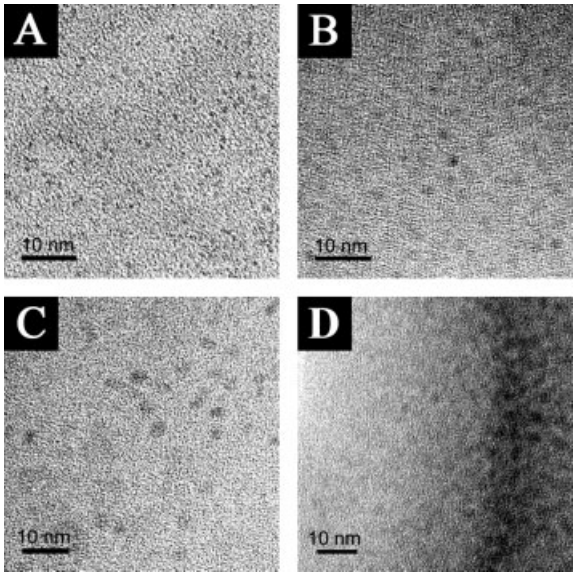

Figure 1. HRTEM images of ZnO(PEGME350) nanoparticles, with synthetic molar ratios [LiOH]/[Zn] for the samples of: A) 3.5, B) 1.4, and C) 1.0; sample D was obtained by heating sample C at 60 °C for 24 h.

are about 1.0, 2.5, 3.5, and 4.0 nm. The molar ratios of [LiOH]/[Zn] used to synthesize samples A, B, and C were 3.5, 1.4, and 1.0, respectively; sample D was prepared by aging sample C at 60 °C for 24 h. It is clear that, within a certain range, the higher the [LiOH]/[Zn] ratio, the smaller the ZnO(PEGME) nanoparticles are, indicating that excess LiOH can prevent ZnO(PEGME) from growing. Aging at elevated temperatures accelerated the growth of ZnO nanoparticles, but it also caused nanoparticle aggregation, emission spectrum red-shift, and quantum yield drop, as discussed later for sample D. Hence, to control the nanoparticle diameters, adjusting the reaction conditions is preferable to post-treating the products.

IR techniques were employed to analyze the raw materials, intermediate products, and final products of the sol–gel reactions. The results are compared with the IR spectra of ZnO(Ac) nanoparticles, as shown in Figure 2. The right-hand side shows a magnification of the range ~1800–1200 cm^{-1} from the left-hand side. After oxidation of PEGME (Fig. 2a), the resulting

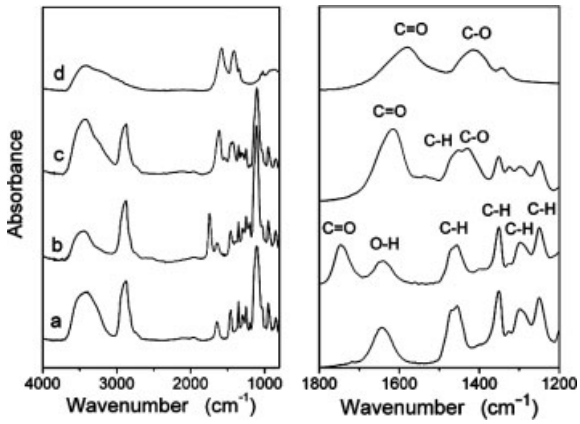

Figure 2. IR spectra of a) PEGME, b) $CH_3O(CH_2CH_2O)_nCH_2COOH$, c) ZnO(PEGME) nanoparticles, and d) ZnO(Ac) nanocrystals. The spectra are shown in more detail (wavenumber region ≈1800–1200 cm^{-1}) on the right-hand side.

$CH_3O(CH_2CH_2O)_nCH_2COOH$ (Fig. 2b) shows a C=O vibration of the COOH group. Compared to Figure 2b, Figure 2c displays two new bands at 1605 and 1440 cm^{-1}, respectively. These new bands are ascribed to the C=O and C–O vibrations of the $CH_3O(CH_2CH_2O)_nCH_2COO^-$ groups on the ZnO(PEGME) nanoparticle surface. Similar C=O and C–O vibration bands were also observed for ZnO(Ac) nanoparticles, as shown in Figure 2d, but the former exhibited a bridging manner, while the latter showed a unidentate form.[8,10] Therefore, IR analyses prove that $CH_3O(CH_2CH_2O)_nCH_2COO^-$ groups were modified covalently on the ZnO surface, just like Ac^- on the ZnO(Ac) nanoparticle surface. Such structural merits substantially distinguish the ZnO(PEGME) nanocomposites from (PEG + ZnO) physical mixtures, and thus their properties are naturally superior to the latter.

The compositions of purified ZnO(PEGME) hybrids made from PEGME with different molecular weights were measured by thermogravimetric analysis (TGA), as shown in Figure 3. All samples begin to decompose at about 400 °C, higher than the PEO decomposition temperature at around 300 °C,[11] indicating

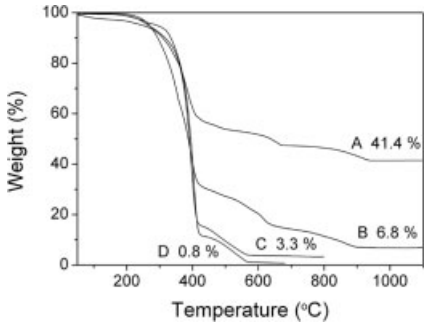

Figure 3. TG curves for ZnO(PEGME) nanoparticles. The samples lose their PEGME surface groups at about 400 °C and the OH groups at higher temperatures. Samples A, B, C, and D were derived from PEGME350, PEGME750, PEGME2000, and PEGME5000, respectively.

ADVANCED FUNCTIONAL MATERIALS

that they have better thermal stabilities. The hybrids lost most of their weight (PEGME surface groups) at about 400 °C, and then lost a little weight slowly, suggesting the loss of the OH groups and chemically adsorbed H_2O molecules.[12] It is clear that the larger the PEGME molecular weight, the smaller the remaining ZnO composition was, identical with the titration analyses. The ZnO composition in the ZnO(PEGME) hybrids directly influences its states and properties. ZnO(PEGME350) behaves quite differently from PEGME350 because it contains 41.4 wt.-% ZnO, while ZnO(PEGME5000) is similar to PEGME5000 because there is only 0.8 wt.-% ZnO in ZnO(PEGME5000). The states of the purified ZnO(PEGME) hybrids at room temperature are dependent on the molecular weights of PEGME raw materials, that is, ZnO(PEGME350) and ZnO(PEGME550) are transparent gels, while ZnO(PEGME750), ZnO(PEGME2000), and ZnO(PEGME5000) are waxes. This type of hybrid can be dissolved by many organic solvents, such as ethanol, toluene, acetonitrile, and chloroform, to form stable colloids with tunable PL from blue to yellow, while the conventional ZnO(Ac) powder cannot be re-dispersed into any solvent.

Figure 4a is a picture of ZnO(PEGME350) colloids under 254 nm UV light. The emission color of the colloids was tuned by adjusting the [LiOH]/[Zn] molar ratio and aging conditions. These samples were diluted to [Zn] = 0.001 M for quantum-

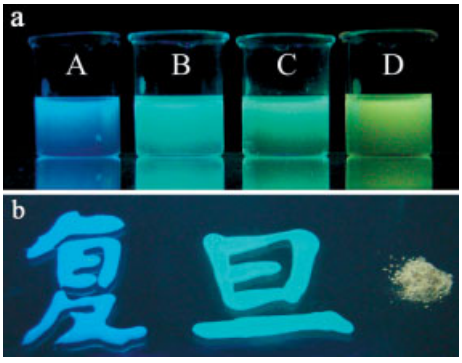

Figure 4. Photographs of ZnO samples under 254 nm UV light. a) ZnO(PEGME350) ethanol colloids prepared under different conditions. Samples A–D are the same as those in Figure 1. b) Purified ZnO(PEGME350) gels of sample A and sample B (Chinese words representing Fudan University) are coated on a piece of glass, together with purified ZnO(Ac) powder. The gels are transparent, with some small bubbles in them.

yield evaluation, and samples A–D showed 29, 31, 27, and 18 %, respectively, much higher than the reported data, ~1–16 %, for the conventional ZnO nanoparticles.[13] Comparison with the HRTEM images in Figure 1 clearly shows that the larger the ZnO nanoparticles, the longer their emission wavelengths are. After purification by the non-solvent method, our new route can prepare blue and green transparent gels, while the traditional ways[8,10,13] only produce a yellow powder under UV irradiation, as shown in Figure 4b. The ZnO(PEGME350) gels are obviously much brighter than the ZnO(Ac) powder, because in the former ZnO nanoparticle cores are protected by the polymer groups, while in the latter the ZnO nanoparticles are highly agglomerated.

It is well-known that, for ZnO nanoparticles, the PL excitation peak position λ_{ex} and the onset λ_{onset} or half-peak position $\lambda_{1/2}$ of UV absorption have direct relationships with the ZnO particle diameters.[14,15] These relationships are given by Equation 1

$$1240/\lambda = a + b/D^2 - c/D \quad (1)$$

where λ can be λ_{ex}, λ_{onset}, or $\lambda_{1/2}$, and a, b, and c are parameters when the ZnO diameter D is within the range ~2.5–6.5 nm.[15] Although this equation is not adequate for calculating an accurate value of D when the λ data are provided by spectral measurements, it is definite that λ increases as D increases if the ZnO particle diameter is in the quantum size region. That is, the UV absorption spectra and PL excitation spectra red-shift when the ZnO nanoparticles grow larger. However, the visible emission of ZnO nanocrystals is much more complicated than the excitation spectra and the UV absorption. According to previous research,[16] ZnO visible luminescence results from the transition of the photogenerated electrons/excitons from a level near the conduction band to some deep traps. The emission wavelength is determined by the energy gap, ΔE, between the initial level and the deep traps. Strangely, ΔE values were found to be very similar in the literature,[13–18] even if ZnO particle diameter changed from 2 to 8 nm, i.e., only green emission could be observed for the fresh ZnO colloids, while yellow samples were usually prepared by firing ZnO films above 150 °C[17] or aging ZnO colloids for days.[18] Not until recently was blue emission observed from ZnO nanoparticles, prepared in highly diluted solutions at around 0 °C,[19] but the blue emission was not stable at room temperature. Contemporarily, Abdullah and co-workers synthesized blue ZnO nanoparticles in a PEO matrix and evaluated the ZnO average diameter to be 4.3 nm according to the Equation 1, but they failed to observe these blue ZnO under TEM.[9b] In fact, the blue ZnO nanoparticles were much smaller than the calculated value. They cannot be 4.3 nm, because 4.3 nm ZnO nanoparticles are usually green–yellow under UV irradiation. As seen in Figure 1A, the blue ZnO nanoparticles are only about 1 nm, invisible under a TEM operated at 100 kV.[9b] Figure 5 exhibits the PL spectra for ZnO(PEGME350) colloids corresponding to the samples in Figure 1, where ZnO excitation spectra and emission spectra

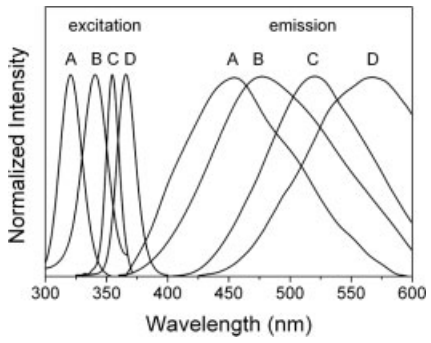

Figure 5. PL spectra of ZnO(PEGME350) colloids. Samples A–D are equivalent to those labelled A–D in Figures 1,4.

red-shifted as the ZnO particle size increased from 1 to 4 nm. Therefore, the goal of tuning ZnO visible luminescence at room temperature simply by controlling particle size, as for CdSe and CdTe,[20] has been realized successfully in the present work.

In order to compare the PL stability of the ZnO(PEGME350) colloids and the (PEGME + ZnO) physical mixture, two typical solutions were prepared and measured from the first hour to the fifteenth day. The PL data are shown in Figure 6. Sample A is composed of 0.01 M $[CH_3O(CH_2CH_2O)_nCH_2COO]_2Zn$ and 0.035 M LiOH; sample B consists of 0.01 M $ZnAc_2$, 0.035 M LiOH, and 1.2 g L^{-1} PEGME350. For the sake of comparison,

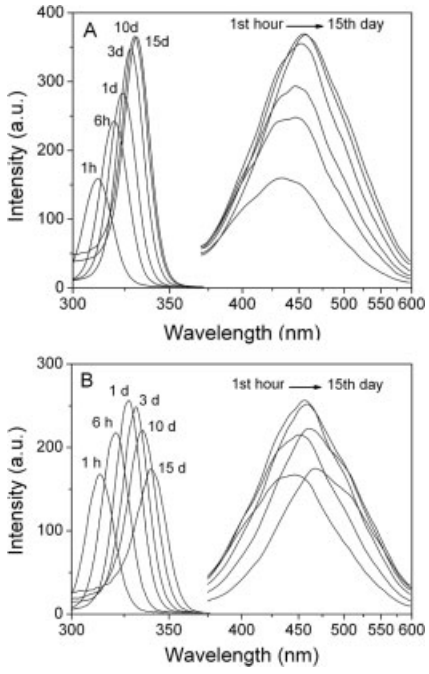

Figure 6. PL spectral evolution along with storage time for two ethanol colloids. Sample A results from 0.01 M $[CH_3O(CH_2CH_2O)_nCH_2COO]_2Zn$ and 0.035 M LiOH; sample B was made from 0.01 M $ZnAc_2$, 0.035 M LiOH, and 1.2 g L^{-1} PEGME350.

the concentration of PEGME molecules in sample B is the same as that of PEGME groups in sample A according to ZnO(PEGME350) composition analyses. The addition of PEGME molecules had little effect on the growth and aggregation of the ZnO(Ac) colloid. The PL intensity of sample B increased in the growth stage (duration approximately one day) and decreased in the following days. The excitation/emission peaks of sample B red-shift and broaden continuously during the storage time, accompanied by Ostwald ripening[21] and precipitation. In contrast, sample A is much more stable. After slow growth in the first three days, the PL spectra change little in the following days, and the stable PL intensity is about two times stronger than that of sample B, indicating the chemically bonded PEGME surface groups can effectively prevent ZnO nanoparticle growth and aggregation. This experiment is excellent proof that the polymer nanocomposite prepared by chemical reactions is much more stable than its counterpart from physical mixing.

Nanoparticle-oxide-doped polymer electrolytes have enhanced conductivity, mechanical properties, and electrochemical stability,[22] but suffer from the instability caused by thermal treatment.[23] This is because the interactions between nanoparticle fillers and solid polymer electrolytes (SPEs) are not strong enough to suppress the crystallization of the composite electrolytes. Bonding small PEO molecules with nanoparticles is an effective way to improve such interactions, and the properties of such polyether-grafted nanoparticles can be easily tuned by changing their compositions and structures. In our previous work,[12] the composites of $LiClO_4$ and PEGME-modified SnO_2 nanoparticles exhibited conductivities above 10^{-5} S cm^{-1} at room temperature, but their powder form limited their applications in electrical devices such as lithium batteries. This provided the motivation to design ZnO(PEGME) in the present work. After dissolving 20 wt.-% $LiN(CF_3SO_2)_2$ in the new nanocomposite, the obtained electrolytes are gels or waxes at room temperature. Thus, it is no longer necessary to blend them with high-molecular-weight PEO for characterization. In Figure 7, the conductivities of the as-prepared hybrid electrolytes are compared with their prototypes during heating scans. The

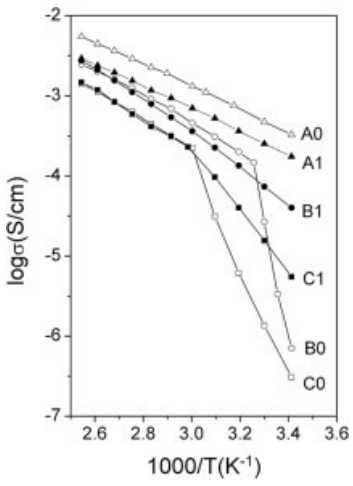

Figure 7. Conductivities (σ) of different samples in the heating scan. These electrolytes are made of 20 wt.-% $LiN(CF_3SO_2)_2$ with PEGME350 (A0), ZnO(PEGME350) (A1), PEGME750 (B0), ZnO(PEGME750) (B1), PEGME5000 (C0), and ZnO(PEGME5000) (C1), respectively.

conductivity of ZnO(PEGME350)–$LiN(CF_3SO_2)_2$ at 20 °C is about 2×10^{-4} S cm^{-1}, a little smaller than that of PEGME350–$LiN(CF_3SO_2)_2$ liquid electrolyte because there is a large amount of ZnO inert composition in the former. However, the conductivities of ZnO(PEGME750)–$LiN(CF_3SO_2)_2$ and ZnO(PEGME5000)–$LiN(CF_3SO_2)_2$ at room temperature far exceed their counterparts, because the hybrid electrolytes are naturally amorphous while the prototypical ones are semicrystalline at 20 °C. Since the curves for ZnO(PEGME)–$LiN(CF_3$-

ADVANCED FUNCTIONAL MATERIALS

$SO_2)_2$ electrolytes have no melting points, in contrast to the prototypes, these new SPEs are wholly amorphous at room temperature. Annealing ZnO(PEGME)–$LiN(CF_3SO_2)_2$ samples under different conditions has almost no influence on the sample conductivities, so the conductivities of the present SPEs do not depend on their thermal history.

In Figure 8, the conductivities of three typical SPE samples are compared versus storage time. After thermal treatment, the prototypical PEGME750–$LiN(CF_3SO_2)_2$ becomes stable within a few days at 20 °C because it crystallizes relatively quickly. Incorporation of 5 wt.-% ZnO(Ac) nanoparticles as fillers resulted

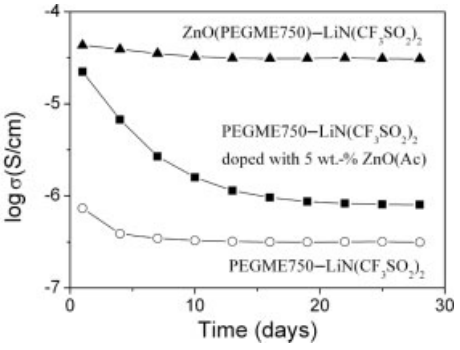

Figure 8. Conductivity evolution at 20 °C versus storage time for the prototypical SPE sample, the ZnO nanofiller-doped sample, and the new SPE sample based on a ZnO(PEGME) hybrid. The $LiN(CF_3SO_2)_2$ content in each sample was 20 wt.-%.

in the crystallization process becoming sluggish, and it took about 25 days for the doped SPE to enter its stable state. This phenomenon is ascribed to the Lewis acid–base interactions between SPE and nanoparticle fillers.[22] Obviously, although doping with nanoparticle fillers could improve the SPE performance, such an improvement, which depends on the thermal history of the sample and usually decays with time, is limited. It can be speculated that ZnO(Ac) nanoparticle fillers aggregate slowly to become larger particles and separate from the as-prepared, uniform polymer–nanoparticle phase, so that the suppressing effects on polymer crystallization from nanoparticle fillers become weaker and weaker. As a result, the conductivity of the nanoparticle-doped SPE decreases slowly, until a new balance is set up between nanoparticle-filler aggregation and polymer crystallization. In contrast, the ZnO(PEGME750)–$LiN(CF_3SO_2)_2$ hybrid is very stable, even though it also contains about 5 wt.-% ZnO nanoparticles and 20 wt.-% lithium salt. Since the polymer component PEGME750 and nanoparticle component ZnO always exist in a common phase (precisely speaking, a solid solution) and the ZnO nanoparticles are prevented from aggregating by the PEGME groups, the suppressing effects on polymer crystallization from nanoparticles will exist forever. Furthermore, better thermal stabilities and electrochemical stabilities can be expected for our new hybrids because of the strong covalent bonds between the ZnO nanoparticle cores and PEGME groups.[12] Experiments to test ZnO(PEGME) hybrids as SPEs in lithium batteries, solar cells, and supercapacitors are underway.

3. Conclusions

We have synthesized a novel type of nanocomposite ZnO-(PEGME), in which ZnO nanoparticles and PEGME polymer groups are connected by covalent bonds, and we have characterized their composition, structure, fluorescence, and conductivity. The results prove that the polymer nanocomposites synthesized by chemical reactions have superior properties compared to those of their counterparts prepared by simple physical mixing. The long-term stability of these properties arises from strong chemical bonds between polymers and nanoparticles. The ZnO(PEGME) hybrids have tunable PL and stable ionic conductivity, indicating their potential for applications in luminescent devices and electronic apparatuses.

4. Experimental

PEGME (0.015 mol; molecular weight = 350, 550, 750, 2000, 5000, Aldrich), $KMnO_4$ (0.02 mol), and NaOH (0.05 mol) were dissolved in water (1 L) by stirring. After reaction for 24 h at room temperature, the resulting MnO_2 precipitate was filtered out, and a colorless transparent solution was obtained. Hydrochloric acid was added to the solution until its pH decreased to about 2.0, and then the solution was evaporated in a rotary evaporator at 70 °C. The solid product was further dried in a vacuum oven at 100 °C to remove all water. The derivative of PEGME, $CH_3O(CH_2CH_2O)_nCH_2COOH$, was obtained by extraction using toluene from the dried product followed by removal of the toluene by rotary evaporation. $CH_3O(CH_2CH_2O)_nCH_2COOH$ was reacted with $Zn(OH)_2$ in hot water to form a $[CH_3O(CH_2CH_2O)_nCH_2COO]_2Zn$ solution. The solution was evaporated and further dried in vacuum at 100 °C, and the product was dissolved in absolute ethanol. Such $[CH_3O(CH_2CH_2O)_nCH_2COO]_2Zn$ ethanol solution was mixed with LiOH ethanol solution to form a ZnO colloid, the concentration of which (marked as [Zn] throughout this paper) was determined by titration using ethylenediaminetetraacetic acid, EDTA, and EBT (EBT: eriochrome black T) at pH 10. The as-prepared ZnO colloid was concentrated by rotary evaporation and precipitated with anhydrous ether (non-solvent method). The precipitate was washed with anhydrous ether repeatedly, and dried to yield a pure ZnO(PEGME) sample.

For HRTEM measurements, a JEM-3010 transmission electron microscope operated at 300 kV was employed. To study the compositions and structures of the samples, the IR spectra were recorded on a Nicolet Impact 410 FTIR spectrometer using KBr pellets; the TGA data were obtained on a Netzsch STA 449C thermal analyzer with a temperature increasing rate of 20 °C min^{-1}. For optical measurements taken with a Perkin–Elmer LS 55 fluorescence spectrophotometer, alcohol solutions containing [Zn] of 0.01 M and different LiOH concentrations were used. To evaluate the quantum yields (QY) [13,24] of the ZnO(PEGME) nanoparticles, quinine sulfate in 0.5 M sulfuric acid (QY = 55 %) was used as a reference for samples emitting blue light, while Rhodamine 6G in ethanol (QY = 95 %) was employed as the reference for samples with green and yellow emission. For electrical tests on a Solartron SI 1287 electrochemical interface and a Solartron SI 1250 impedance/gain-phase analyzer, the purified ZnO(PEGME) and $LiN(CF_3SO_2)_2$ were dissolved in ethanol or acetonitrile and dried to gels or waxes at room temperature. The $LiN(CF_3SO_2)_2$ content in the obtained SPEs was fixed at 20 wt.-%. These electrolyte samples were heated in a 100 °C vacuum oven for 24 h to remove water or solvent thoroughly, and transferred into a glove box where they were sandwiched between two stainless-steel electrodes to test the alternating current (AC) impedance spectra. The scanning frequency was varied from 10^5 to 0.1 Hz, and the applied voltage was fixed at 500 mV. For comparison, ZnO(Ac) col-

loids were added into ZnO(PEGME) and $LiN(CF_3SO_2)_2$ solutions, dried and treated in the same way, to prepare ZnO(Ac)-doped SPE samples.

Received: March 23, 2005
Final version: July 7, 2005
Published online: September 5, 2005

[1] a) V. F. Puntes, K. M. Krishnan, A. P. Alivisatos, *Science* **2001**, *291*, 2115. b) Y. Cui, Q. Wei, H. Park, C. M. Lieber, *Science* **2001**, *293*, 1289. c) Z. W. Pan, Z. R. Dai, Z. L. Wang, *Science* **2001**, *291*, 1947. d) P. Yang, D. Zhao, D. I. Margolese, B. F. Chmelka, G. D. Stucky, *Nature* **1998**, *396*, 152. e) P. Poizot, S. Laruelle, S. Grugeon, L. Dupont, J.-M. Tarascon, *Nature* **2000**, *407*, 496. f) N. Sata, K. Eberman, K. Eberl, J. Maier, *Nature* **2000**, *408*, 946.

[2] a) M. Templin, A. Franck, A. D. Chesne, H. Leist, Y. Zhang, R. Ulrich, V. Schädler, U. Wiesner, *Science* **1997**, *278*, 1795. b) F. Caruso, R. Caruso, H. Möhwald, *Science* **1998**, *282*, 1111. c) A. Sellinger, P. M. Weiss, A. Nguyen, Y. Lu, R. A. Assink, W. Gong, C. J. Brinker, *Nature* **1998**, *394*, 256. d) A. K. Boal, F. Ilhan, J. E. DeRouchey, T. Thurn-Albrecht, T. P. Russell, V. M. Rotello, *Nature* **2000**, *404*, 746. e) W. U. Huynh, J. J. Dittmer, A. P. Alivisatos, *Science* **2002**, *295*, 2425.

[3] a) F. Caruso, H. Lichtenfeld, M. Giersig, H. Möhwald, *J. Am. Chem. Soc.* **1998**, *120*, 8523. b) M. J. MacLachlan, I. Manners, G. A. Ozin, *Adv. Mater.* **2000**, *12*, 675. c) R. Gangopadhyay, A. De, *Chem. Mater.* **2000**, *12*, 608. d) R. Shenhar, T. B. Norsten, V. M. Rotello, *Adv. Mater.* **2005**, *17*, 657.

[4] a) A. Imhof, *Langmuir* **2001**, *17*, 3579. b) F. Caruso, *Adv. Mater.* **2001**, *13*, 11. c) M. M. Sigalas, W. Zubrzycki, S. R. Kurtz, J. Bur, *Nature* **1998**, *394*, 251. d) J. Marti, V. G. Ralchenko, *Science* **1998**, *282*, 897.

[5] a) E. P. Giannelis, *Adv. Mater.* **1996**, *8*, 29. b) L. Wang, M. Rocci-Lane, P. Brazis, C. R. Kannewurf, Y. Kim, W. Lee, J. Choy, M. G. Kanatzidis, *J. Am. Chem. Soc.* **2000**, *122*, 6629. c) D. J. Chaiko, *Chem. Mater.* **2003**, *15*, 1105. d) S. K. Lim, J. W. Kim, I. Chin, Y. K. Kwon, H. J. Choi, *Chem. Mater.* **2002**, *14*, 1989.

[6] a) F. Croce, G. B. Appetecchi, L. Persi, B. Scrosati, *Nature* **1998**, *394*, 456. b) L. Qi, H. Cölfen, M. Antonietti, *Nano Lett.* **2001**, *1*, 61. c) R. A. Vaia, S. Vasudevan, W. Krawiec, L. G. Scanlon, E. P. Giannelis, *Adv. Mater.* **1995**, *7*, 154. d) V. Bekiari, P. Lianos, U. L. Stangar, B. Orel, P. Judeinstein, *Chem. Mater.* **2000**, *12*, 3095.

[7] a) M. S. Lavine, *Science* **2004**, *303*, 927. b) H. Zhang, Z. Cui, Y. Wang, K. Zhang, X. Ji, C. Lü, B. Yang, M. Gao, *Adv. Mater.* **2003**, *15*, 777. c) J. Lee, V. C. Sundar, J. R. Heine, M. G. Bawendi, K. F. Jensen, *Adv. Mater.* **2000**, *12*, 1102. d) J. Y. Wang, W. Chen, A. H. Liu, G. Lu, G. Zhang, J. H. Zhang, B. Yang, *J. Am. Chem. Soc.* **2002**, *124*, 13 358.

[8] H. M. Xiong, X. Zhao, J. S. Chen, *J. Phys. Chem. B* **2001**, *105*, 10 169.

[9] a) M. Abdullah, M. Tsutomu, K. Okuyama, *Adv. Funct. Mater.* **2003**, *13*, 800. b) M. Abdullah, I. W. Lenggoro, K. Okuyama, F. G. Shi, *J. Phys. Chem. B* **2003**, *107*, 1957.

[10] S. Sakohara, M. Ishida, M. A. Anderson, *J. Phys. Chem. B* **1998**, *102*, 10 169.

[11] a) T. Shodai, B. B. Owens, H. Ohtsuka, J. Yamaki, *J. Electrochem. Soc.* **1994**, *141*, 2978. b) H. M. Xiong, J. S. Chen, D. M. Li, *J. Mater. Chem.* **2003**, *13*, 1994.

[12] H. M. Xiong, D. P. Liu, H. Zhang, J. S. Chen, *J. Mater. Chem.* **2004**, *14*, 2775.

[13] a) D. W. Bahnemann, C. Kormann, M. R. Hoffmann, *J. Phys. Chem.* **1987**, *91*, 3789. b) M. Schubnell, I. Kamber, P. Beaud, *Appl. Phys. A: Mater. Sci. Process.* **1997**, *64*, 109. c) A. V. Emeline, V. K. Ryabchuk, N. Serpone, *J. Phys. Chem. B* **1999**, *103*, 1316.

[14] a) G. Redmond, A. O'Keeffe, C. Burgess, C. MacHale, D. Fitzmaurice, *J. Phys. Chem.* **1993**, *97*, 11 081. b) M. Haase, H. Weller, A. Henglein, *J. Phys. Chem.* **1988**, *92*, 482.

[15] a) E. A. Meulenkamp, *J. Phys. Chem. B* **1998**, *102*, 5566. b) E. A. Meulenkamp, *J. Phys. Chem. B* **1998**, *102*, 7764.

[16] a) A. van Dijken, E. A. Meulenkamp, D. Vanmaekelbergh, A. Meijerink, *J. Lumin.* **2000**, *89*, 454. b) A. van Dijken, E. A. Meulenkamp, D. Vanmaekelbergh, A. Meijerink, *J. Lumin.* **2000**, *90*, 123. c) A. van Dijken, E. A. Meulenkamp, D. Vanmaekelbergh, A. Meijerink, *J. Phys. Chem. B* **2000**, *104*, 1715.

[17] S. Sakohara, L. D. Tickanen, M. A. Anderson, *J. Phys. Chem.* **1992**, *96*, 11 086.

[18] L. Spanhel, M. A. Anderson, *J. Am. Chem. Soc.* **1991**, *113*, 2826.

[19] A. Wood, M. Giersig, M. Hilgendorff, A. Vilas-Campos, L. M. Liz-Marzan, P. Mulvaney, *Aus. J. Chem.* **2003**, *56*, 1051.

[20] a) M. Bruchez, M. Moronne, P. Gin, S. Weiss, A. P. Alivisatos, *Science* **1998**, *281*, 2013. b) X. Peng, J. Wickham, A. P. Alivisatos, *J. Am. Chem. Soc.* **1998**, *120*, 5343. c) H. Zhang, L. P. Wang, H. M. Xiong, L. H. Hu, B. Yang, W. Li, *Adv. Mater.* **2003**, *15*, 1712.

[21] a) W. Z. Ostwald, *Phys. Chem.* **1901**, *37*, 385. b) E. V. Shevchenko, D. V. Talapin, A. L. Rogach, A. Kornowski, M. Haase, H. Weller, *J. Am. Chem. Soc.* **2002**, *124*, 11 480. c) D. V. Talapin, A. L. Rogach, M. Haase, H. Weller, *J. Phys. Chem. B* **2001**, *105*, 12 278.

[22] a) T. Abe, M. Ohtsuka, F. Sagane, Y. Iriyama, Z. Ogumi, *J. Electrochem. Soc.* **2004**, *151*, A1950. b) D. Swierczynski, A. Zalewska, W. Wieczorek, *Chem. Mater.* **2001**, *13*, 1560. c) F. Croce, R. Curini, A. Martinelli, L. Persi, F. Ronci, B. Scrosati, R. Caminiti, *J. Phys. Chem. B* **1999**, *103*, 10 632. d) E. Quartarone, P. Mustarelli, A. Magistris, *Solid State Ionics* **1998**, *110*, 1.

[23] a) J.-M. Tarascon, M. Armand, *Nature* **2001**, *414*, 359. b) B. Kumar, S. Koka, S. J. Rodrigues, M. Nookala, *Solid State Ionics* **2003**, *156*, 163. c) H. M. Xiong, K. K. Zhao, X. Zhao, Y. W. Wang, J. S. Chen, *Solid State Ionics* **2003**, *159*, 89.

[24] L. Qu, X. Peng, *J. Am. Chem. Soc.* **2002**, *124*, 2049.

